Enhancing Poxvirus Oncolytic Effects through Increased Spread and Immune Evasion

David H. Kirn,[1] Yaohe Wang,[2] Wenchung Liang,[3] Christopher H. Contag,[3] and Stephen H. Thorne[4]

[1]Jennerex Biotherapeutics, Ltd., San Francisco, California; [2]Cancer Research UK Molecular Oncology Center, Queen Mary's School of Medicine and Dentistry, Charterhouse Square, London, United Kingdom; [3]Department of Pediatrics, Microbiology and Immunology and Radiology and Bio-X Program, Stanford University, Stanford, California; and [4]Department of Surgical Oncology, University of Pittsburgh, Pittsburgh, Pennsylvania

Abstract

The antitumoral effects of oncolytic viruses have generally been limited by inefficient spread of the viruses within infected tumors and by inefficient systemic delivery, particularly in preimmunized hosts. Tumor-selective poxviruses have biological characteristics that may overcome these limitations. Nevertheless, physical barriers within the tumor microenvironment, including the extracellular matrix, can still limit intratumoral spread, and neutralizing antibodies can impede systemic delivery. To counter these limitations, we sought to take advantage of a naturally occurring poxvirus form known as extracellular enveloped virus (EEV). The EEV is shrouded by a host cell–derived lipid bilayer containing anticomplement proteins and is typically released from infected cells early during the infection cycle. Therefore, the EEV form evolved for rapid systemic spread within the host and for evasion of immune-mediated clearance. We compared the oncolytic potential of low versus high EEV-producing strains of vaccinia. EEV-enhanced vaccinia strains displayed improved spread within tumors after systemic delivery, resulting in significantly improved antitumor effects. The EEV-enhanced strains also displayed a greater ability to spread between injected and noninjected distant tumors through the blood and, importantly, displayed reduced clearance by neutralizing antibody. Safety was unaffected. The incorporation of EEV-enhancing mutations into next generation oncolytic vaccinia strains may improve the potency of these viruses without sacrificing safety. [Cancer Res 2008;68(7):2071–5]

Introduction

Oncolytic viruses, whose replication has been restricted to malignant cells, represent promising anticancer agents (1, 2). We have recently shown that genetically modified strains of vaccinia virus are capable of local or systemic delivery to tumors resulting in significant antitumor effects in preclinical models (3, 4). This is in part due to the evolved ability of poxviruses to travel within the blood of a host largely undetected. To achieve this, vaccinia has evolved distinct viral forms produced at different stages of its life cycle; these include the intracellular virus and the enveloped virus (5, 6). The enveloped virus may further exist as cell-associated enveloped virus (CEV) or extracellular enveloped virus (EEV). Enveloped virus is produced early after infection of a susceptible cell

and is released from the cell before lysis, leading to rapid spread of the virus within the host. While the CEV form remains tethered to the infected cell, inducing an actin tail beneath it that acts to propel the virus toward neighboring cells, the EEV form is released from the infected cell and so is able to spread systemically within a host. The extra lipid bilayer that defines the enveloped virus is provided by the host cell with only one antigenic viral protein exposed on the surface of the enveloped virus, making it relatively resistant to complement or antibody-mediated neutralization (7, 8). Mutations that reduce the levels of enveloped virus produced from an infected cell are highly attenuating, reflecting the importance of this form of the virus for spread within a host. In addition, a variety of vaccinia mutations that increase the percentage of the enveloped virus that is released from the host cell (as EEV) relative to the amount that remains cell-associated (as CEV; refs. 9–12) have been described. These mutations, despite enhancing systemic spread, do not increase the pathogenicity of the virus.

We therefore sought to determine whether such EEV enhancing mutations would be beneficial in the context of an oncolytic strain of vaccinia. We found that increasing the relative levels of EEV produced during the viral life cycle enhanced the spread of the virus in three-dimensional tissue culture systems and increased the early intratumoral spread of the virus after systemic delivery in mouse tumor models. This led to enhanced antitumoral efficacy. We also showed that mutations that increased EEV production produced an oncolytic virus more efficient at spreading between tumors through the blood. Finally, the EEV enhancement was also capable of dramatically improving the systemic spread of the virus in the face of neutralizing antibody. Safety in tumor-bearing models was unchanged. The incorporation of EEV enhancing mutations into next generation oncolytic strains of vaccinia virus will therefore likely enhance their therapeutic benefit without affecting safety and may act to allow repeat treatments even in the face of antiviral immune neutralizing antibodies.

Materials and Methods

Cell lines and viruses. The cell lines PC3 (human prostate cancer) and 4T1 (murine mammary cancer, BALB/c) were obtained from American Type Culture Collection (ATCC), and the cell lines CMT 64 (murine lung cancer, C57/BL6) and JC (murine mammary cancer, BALB/c) were provided by Cancer Research UK cell bank. All cell lines were cultured in DMEM with 10% bovine serum. The Western Reserve (WR) virus was obtained from ATCC; the IHD-J and A5L-GFP (containing a fusion between the A5L gene and GFP; ref. 13) viruses were kindly provided by Geoffrey Smith (Imperial College); the WI virus (WR virus with the A34R gene from IHD-J recombined into the WR A34R gene locus; ref. 14) was kindly provided by Bernard Moss (NIH); the WR TK-Luc+ virus was kindly provided by David Bartlett (University of Pittsburgh). The WR TK-GFP+ strain was described previously (15). Additionally, modified pSC-65 plasmid expressing firefly luciferase (Promega) from under control of the pSE/L promoter was used to insert

luciferase into the site of the thymidine kinase gene of the WI virus, creating a WR A34R(IHD-J) TK-Luc+ virus.

Three-dimensional tissue culture spheroids. PC3 cells growing as an adherent monolayer were trypsinized and transferred to untreated tissue culture plates and examined microscopically daily. Typically, cells began to clump together 12 to 24 h after transfer, and by 48 to 72 h, cells had formed tightly associated symmetrical tumor spheroids. Individual spheroids were surface stained with cell tracker Orange (Invitrogen), transferred to wells of chamber slides (Labtek), and mixed with virus expressing GFP, as indicated. At times after viral addition, individual spheroids were imaged by confocal microscopy and Z-stack images were reconstructed into three-dimensional models (Velocity software). Individual Z-stack images were also used to delineate the outer surface of the spheroid (from cell tracker staining) and the amount of the inner area that was green (GFP positive) to determine the percentage of the spheroid infected with virus (calculated using Velocity software).

Mouse tumor models. Female mice (ages 8–10 wk) were implanted s.c. with different tumor cell lines. CMT 64 cells (1×10^5) were implanted into C57/BL6 mice, 1×10^5 JC cells were implanted into BALB/c (s.c. hind flank), and tumors were allowed to form for 10 to 14 d until palpable (50–100 mm³). Animals were then treated with a single i.v. (tail vein) injection of virus at indicated doses. Effects on tumor growth were determined by caliper measurement, and animals were removed from the study when their tumor volume reached 1.44 cm³. In addition, further animals were sacrificed at predetermined times after treatment for recovery of tumor tissue for histologic analysis.

In other experiments, BALB/c mice were injected with 1×10^4 4T1 cells into the mammary fatpad. In this model, primary tumors were determined to reliably metastasize to the lungs between 7 and 10 d after initial implantation (data not shown). Animals were treated with 1×10^7 plaque-forming units (pfu) of vaccinia virus strains expressing luciferase via i.t.
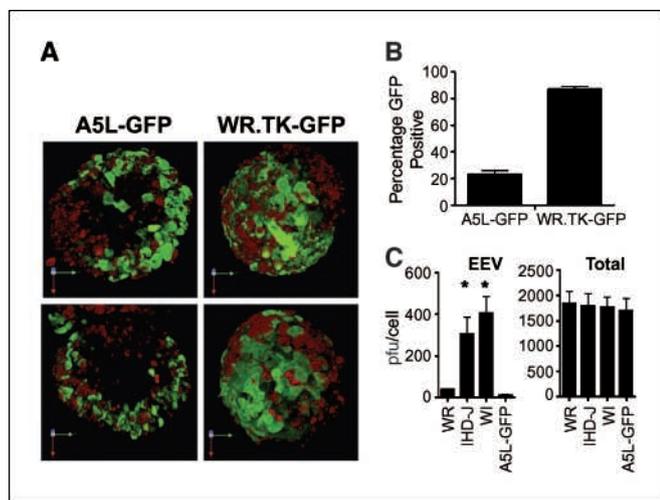

Figure 1. Spread of vaccinia strains in three-dimensional tissue culture models. *A,* PC3 (human prostate cancer) cells were used to form multicellular tumor spheroids in tissue culture and then labeled with cell tracker and were treated with vaccinia strains WR TK-GFP+ (normal EEV production) or A5L-GFP fusion (low EEV production; 500 pfu/spheroid). Subsequent viral gene expression (*green*) within the spheroid (*red*) was determined by confocal fluorescence microscopy 72 h after infection; I and II represent two independent spheroids receiving the same treatment. At 72 h, a number of the labeled cells on the outer surface have been lysed or shed from the spheroid, leading to irregular staining. *B,* analyses of the percentage of the spheroids expressing GFP (as determined on Velocity software; see Materials and Methods) 72 h after viral treatment ($n = 5$; $P < 0.0001$). *C,* analysis of release of virus into the media at early times after infection of a PC3 monolayer. PC3 cells grown as an adherent monolayer were infected with vaccinia strains WR, IHD-J, WI, or A5L-GFP (5 pfu/cell). Media were collected 24 h after infection, and virus released into the media titered (EEV). *, values for IHD-J ($P = 0.0289$) and WI ($P = 0.0104$) are significantly greater than for WR. Alternatively, overall virus production was titered. *Total,* combined media, cell-associated, and intracellular virus.
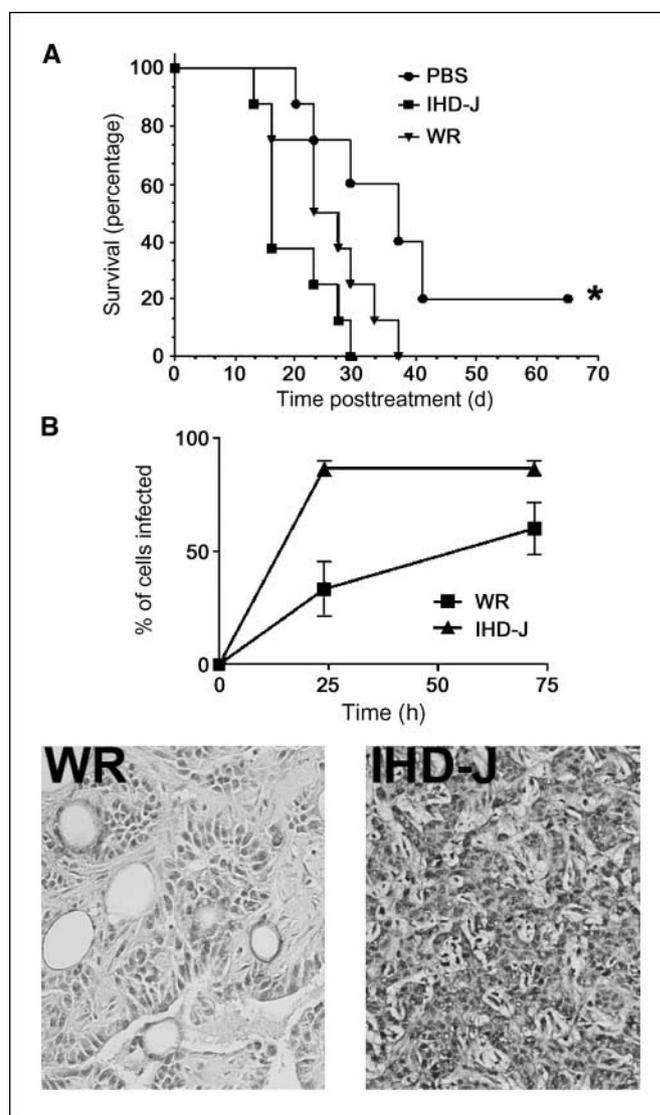

Figure 2. *A,* survival of tumor-bearing mice after treatment with different vaccinia strains. C57/BL6 mice implanted with subcutaneous CMT 64 tumors (50–100 mm³) were treated with a single tail vein injection of 1×10^6 pfu of vaccinia strain IHD-J or WR, or PBS as a control. Subsequent survival (Kaplan-Meier) was followed ($n = 8$). *, IHD-J displayed significantly increased survival relative to WR ($P = 0.0248$). *B,* spread of virus within the tumor microenvironment. Mice were treated as above and sacrificed at indicated times after treatment ($n = 3$ per time point), and tumors were excised for immunohistochemistry for viral coat protein. Histopathology scoring for positive staining was performed blinded on 10× high-power field of view per tumor and for three mice at each treatment time point. Representative pictures at 24 h after treatment (40×).

injection into the primary tumor 14 d after implantation, and viral biodistribution was followed by bioluminescence imaging (BLI). In some experiments, animals were treated with vaccinia immunoglobulin (VIG; 250 mg/kg delivered via i.p. injection) 24 h before viral treatment. Blood samples were obtained to determine the levels of circulating antibody within the serum by vaccinia neutralization assay (4).

All animal studies were performed according to institutionally approved animal protocols.

Immunohistochemistry and immunofluorescence. For immunohistochemistry studies, organs were fixed in formalin before embedding in paraffin blocks for sectioning. Sections were stained with H&E and for viral coat proteins (polyclonal antivaccinia antibody). Average numbers of positive cells per high-power field (40×) from an average of 10 randomly

chosen fields from each of three mice treated under each condition at each time point were determined by blinded analysis.

For immunofluorescence studies, tumors from mice treated with vaccinia strains were frozen in optimal cutting temperature compound and sectioned (8–10 μm). Tissue slices were fixed in acetone, blocked with 2% FCS and stained using labeled antibodies to CD31 or vaccinia virus (Invitrogen, Molecular Probes), as indicated, and nuclear staining with Sytox Blue (Invitrogen, Molecular Probes). Sections were then examined using a Leica Confocal microscope.

BLI. Mice received luciferin and were anesthetized (3% isoflurane) and imaged in an IVIS100 imaging system (Xenogen, part of Caliper Life Sciences). Images were analyzed with Living Image software (Xenogen, part of Caliper Life Sciences). Regions of interest were placed around the lungs (upper abdomen) or tumors of imaged animals, and bioluminescent flux $(Ph/s/Sr^2/cm^2)$ was determined for both regions.

Statistical analysis. Groups were compared using two-tailed Student's t test, other than survival curves that were compared by Wilcoxon analyses. A P value of <0.05 was considered significant.

Results

We initially sought to determine how the EEV form of vaccinia virus contributed to viral spread within a three-dimensional tumor model system in tissue culture. Multicellular tumor spheroids, containing ~2,000 PC3 cells per spheroid were mixed with vaccinia strains expressing GFP (500 pfu/spheroid). The WR TK-GFP+ strain replicates normally in culture, whereas the A5L-GFP virus is known to have an ~3-fold reduction in EEV production (13). We showed that at 48 h after initial infection (Fig. 1), the EEV-producing virus had spread throughout the spheroid, infecting over 80% of the cells, whereas the EEV-reduced virus had only infected 20% of the cells at this time. This highlights the increased oncolytic potential of an early release of infectious viral particles from infected cells.

We therefore sought to enhance the levels of EEV production from vaccinia-infected cells. The IHD-J strain of vaccinia virus is known to produce a large percentage of its enveloped virus form as EEV, whereas the WR strain produces mostly CEV. This is due to a single mutation in the $A34R$ gene (K151Q) in the IHD-J strain, and so we additionally examined a WR strain with the native $A34R$ gene replaced with that from IHD-J (WI; refs. 10, 14). Initial studies confirmed that the rate of release of virus into the media (primarily EEV) after infection of tumor cells was consistent with expected levels of EEV production for the different viral strains (Fig. 1C). The overall levels of virus production for each viral strain were equivalent.

We then compared the spread and oncolytic potential of these viruses in mouse tumor models. Mice bearing subcutaneous CMT 64 tumors were treated with a single tail vein injection of 1×10^7 pfu of IHD-J or WR (or PBS as a control), and survival was subsequently determined (Fig. 2A). The IHD-J (high EEV producers)–treated animals displayed a significant increase in survival relative to WR-treated animals ($P = 0.0248$). To examine whether EEV production from the IHD-J strain was enhancing viral spread within the tumor, animals were sacrificed at times after treatment, and viral distribution within the tumor was examined by immunohistochemistry (Fig. 2B). The IHD-J strain was seen to be capable of very rapid spread throughout the entire tumor (87% of tumor cells infected by 24 h compared with 31% for WR; $P = 0.013$), suggesting that EEV production may enhance early spread within the tumor, allowing the virus to infect a greater percentage of the tumor cells before the initiation of an adaptive antiviral immune response and subsequent viral clearance.

However, as IHD-J and WR are distinct vaccinia strains, other mutations or differences between these viruses might also contribute to their oncolytic potential. We therefore examined the WI strain; this virus has the EEV-enhancing IHD-J mutation in the $A34R$ gene inserted into the WR virus. This viral strain could be directly compared with WR to compare the effects of enhanced EEV production in otherwise identical viruses. In this experiment, an alternative tumor model was used (JC cells implanted s.c. into BALB/c mice) to examine the general applicability of these effects (Fig. 3). Once again, it was found that a significant survival advantage was provided by the EEV-enhanced strain over the wild-type virus ($P = 0.006$), with 50% of the animals treated with the WI strain experiencing complete and durable responses. Again, rapid early viral spread within the tumor, especially in less well-vascularized areas, seemed to correlate with this increased survival (Fig. 3B).

Because the EEV form of the virus has evolved for systemic spread within a host, the ability for EEV enhanced strains to spread between tumors was also examined. As the outer envelope of the enveloped viruses is inherently unstable *ex vivo*, we initially examined the spread of different vaccinia strains from a primary subcutaneous tumor to lung metastases. We have previously characterized a model of metastases involving orthotopic implantation of 4T1 tumor cells into the mammary fatpad, resulting in metastasis to the lungs, bone, and lymph nodes. We therefore delivered different viral strains via direct i.t. injection into the primary fatpad tumor at time points after metastasis has occurred and examined the subsequent appearance and levels of virus in the lung metastases. For this study, we used strains of WR
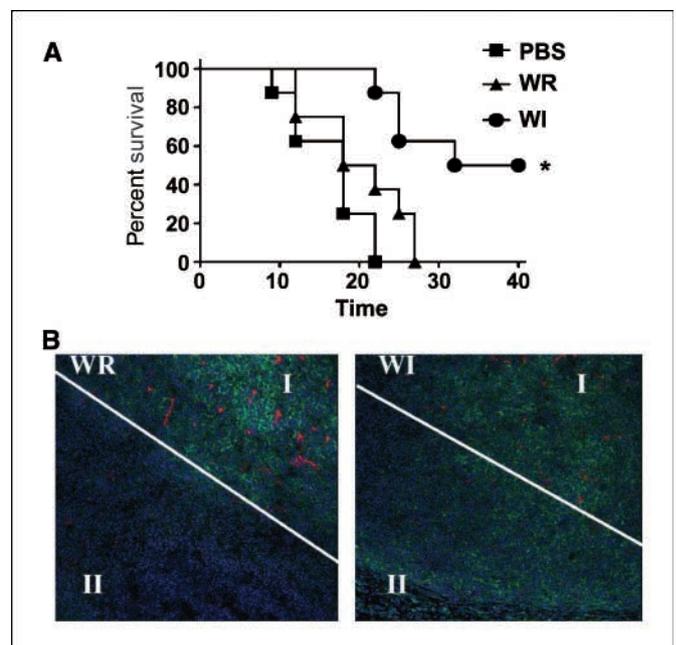

Figure 3. Effects of EEV enhancement on survival and viral spread within the tumor. *A,* survival of BALB/c mice bearing subcutaneous JC tumors (50–100 mm³) after a single tail vein treatment with 1×10^6 pfu of the indicated vaccinia strains (WR, IHD-J, or WI) or PBS control ($n = 8$), *, WI produced significantly greater survival than WR ($P = 0.006$). *B,* tumors from mice treated as above and sacrificed 24 h after treatment were stained for immunofluorescence analysis: sytox blue nuclear stain (*blue*), CD31 (*red*), vaccinia coat protein (*green*). WI strain displayed more complete spread through the tumor and away from initial infection around the vasculature. *I,* vascular region; *II,* poorly vascular region.

[predominantly intracellular mature virus (IMV)] and WI (predominantly EEV) with the firefly luciferase gene expressed from within the locus of the viral thymidine kinase gene. The loss of the thymidine kinase gene is a tumor-targeting, attenuating deletion (16), and the expression of luciferase allowed the detection of viral biodistribution (gene expression) by BLI. In initial studies (Fig. 4), it was found that the WI TK-Luc+ virus displayed significantly enhanced systemic spread from the primary tumor to metastases, primarily within the lungs, but also in the lymph nodes, ribcage, and skull. Secondary spread of the oncolytic viruses was not seen when an alternative breast cancer model was used (JC cells implanted into the fatpad of BALB/c mice), which we have found does not metastasize, implying that the viral gene expression signal from the lungs and other tissues is caused by expression after infection of metastases and not normal tissue. This highlights the previously reported potential of vaccinia strains expressing reporter genes to act as tumor imaging agents (17).

Because the outer, exposed membrane of the enveloped virus is obtained form the host cell and expresses very few viral antigens, it is possible that the EEV form could be used to deliver virus systemically even in the face of an antiviral immune response. In a final set of experiments, we therefore sought to determine whether the EEV virus could avoid neutralizing antibody within the host. As before, because of the impracticality of delivering EEV directly to the animal, we injected viral strains into a primary fatpad 4T1 tumor and measured subsequent spread via levels of viral gene expression signal (bioluminescence) appearing within lung metastases. To distinguish immune-mediated blockade of viral spread (primarily mediated by circulating neutralizing antibodies in an immunized host) and immune clearance of infected cancer cells (primarily by cell-mediated adaptive immune responses), animals were pretreated with VIG. Animals received VIG (250 mg/kg) 24 h before initial infection of the primary tumor and were bled at the time of viral treatment and again at 72 h later (at the time of imaging) to verify maintenance of circulating neutralizing antibody in the serum. It was found that serum from VIG-treated mice had an antibody titer of $1,863 \pm 597$, whereas serum from immunized humans were found to have a mean antibody value of $1,559 \pm 650$ ($n = 4$) using a plaque reduction neutralization assay (naive human serum had a value of 97 ± 32).

Both viruses displayed reduced levels of secondary spread when VIG had been previously given to the animals (Fig. 4B). However, whereas VIG blocked over 90% of the secondary spread of the WR TK-Luc+ strain, the figure was only 60% for the WI strain. This resulted in two logs greater signal within the metastases when the WI TK-luc+ virus was used after VIG delivery relative to WR. It therefore appears that enhancing EEV production provides an opportunity to deliver oncolytic viruses to tumors even in the face of neutralizing antibody, which has traditionally represented a major potential limitation to the clinical use of oncolytic viral strains.

Discussion

The benefits of oncolytic viral therapy should be greatly improved by advances that permit the rapid spread of viruses
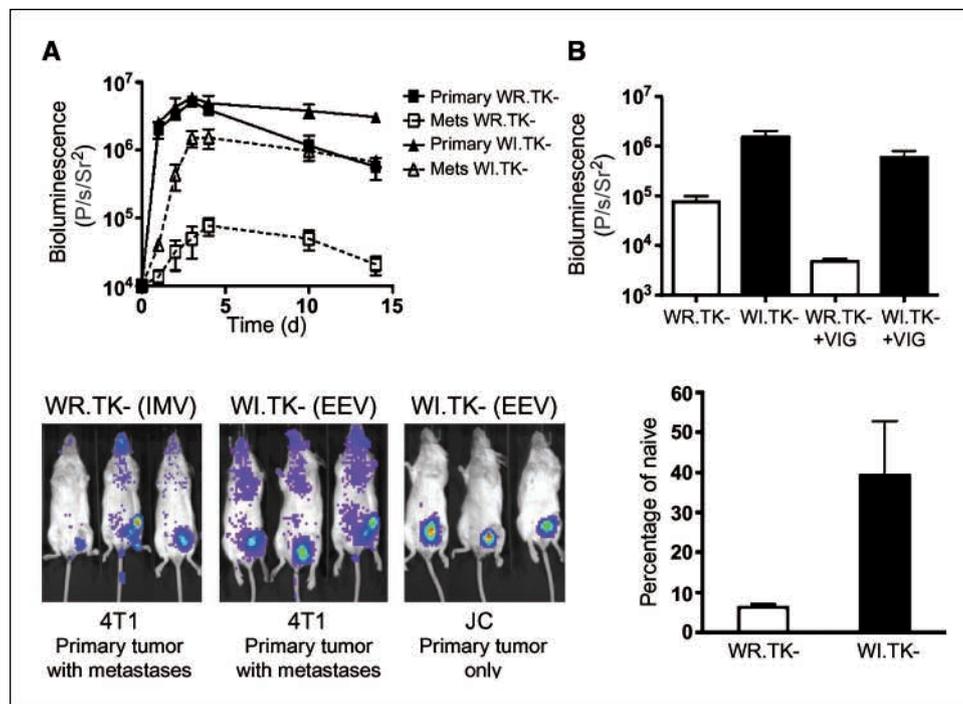

Figure 4. Spread of viral strains between primary tumor and metastases. *A,* mice (BALB/c) bearing 4T1 tumors implanted into the fatpad and allowed to metastasize to the lungs, bone, and lymph nodes were treated with a single i.t. (primary tumor) injection of 1×10^7 pfu of either WR (CEV producing strain) or WI (EEV producing strain); both strains expressed luciferase from the thymidine kinase locus. Viral gene expression was measured at different times by BLI, and regions of interest were drawn over the primary tumor and the lung metastases (upper abdomen). Quantification of the photon flux in these regions was quantified and graphed ($n = 3$). Representative images at 72 h are shown (*bottom*), along with images from mice bearing JC fatpads tumors (which do not metastasize) and treated with WI expressing luciferase. No viral spread was seen when no metastases are present. *B,* this experiment was repeated for mice bearing 4T1 fatpad tumors with metastases and treated with 1×10^7 pfu of WR or WI expressing luciferase via direct i.t. injection 24 h after administration of vaccinia neutralizing antibody (VIG; 250 mg/kg). Levels of bioluminescence detected in the lungs (upper abdomen) 72 h after viral treatment were determined for animals treated with either virus and with or without VIG ($n = 4$). Viral signal within metastatic tumors is also presented normalized relative to non–VIG-treated mice for each virus ($P = 0.04$).

within the complex tumor microenvironment and especially by strategies to overcome limitations imposed on systemic delivery of viral agents by prior antiviral immunization (either due to previous natural exposure, previous immunization, or previous therapy with the same virus). We attempted to enhance the relative production of a naturally occurring form of vaccinia virus that has evolved to spread systemically within an infected host and to evade immune-mediated removal from the blood. This form, known as EEV, is wrapped in a lipid bilayer obtained from the host cell and is released into the blood stream early after infection. A variety of mutations have been described in vaccinia that produce greater relative levels of the EEV form, and previous studies with these strains have found that they either have no effect or slightly reduce the pathogenicity of the virus. We therefore examined the effects of these EEV enhancing mutations on the oncolytic potential of vaccinia strains.

Having initially verified that these strains also displayed enhanced EEV production in tumor cells and established that the early release of enveloped virus was important for viral spread within a three-dimensional tumor model, we examined the effects of EEV-enhancing mutations *in vivo*. Importantly, increased EEV production resulted in greater biodistribution of the virus within the tumor microenvironment, which (as we have found previously; ref. 15) results in a more potent antitumor effect. In addition to improved intratumoral spread, the EEV-enhanced strains also displayed increased intertumoral spread, with more efficient spread of the virus from injected primary tumors to noninjected metastatic tumors. This increases the potential of these viruses to effectively treat dispersed or metastatic disease.

Finally, because a significant portion of the population has previously been vaccinated with vaccinia, as part of the smallpox eradication program or as part of more recent biodefense concerns, and antibodies to IMV and EEV are long living, it may be necessary to deliver oncolytic vaccinia to the tumor in the face of neutralizing antibody. This will also be true if repeat dosing is needed with oncolytic vaccinia to more effectively treat the tumor. Here, we found that the EEV-enhanced strains also permitted more efficient systemic movement of the virus between tumors in the face of high levels of circulating neutralizing antibody. Because the outer envelope of the EEV virus consists primarily of host cell–derived membrane and proteins (including a variety of complement control proteins), it is able to move relatively undetected within the host. The B5R viral protein is the only immune-targeted viral protein exposed on the surface of the EEV (18), and although neutralizing antibodies against this protein are typically produced in an effective immunization, only a small percentage of the antibodies recognize B5R antigens (as the majority of the antibodies produced recognize the more antigenic intracellular virus version of the virus; ref. 19). It is therefore possible that an increased release of EEV into the blood stream will result in some evasion or "swamping" of this neutralizing antibody and systemic spread of the virus to distant tumors. It is also feasible that alterations of the B5R protein may allow the development of antigenically distinct EEV forms of the virus, allowing repeat treatments with slightly altered vaccinia strains.

Currently, however, due to the relative instability of the outer membrane of the EEV form, purification steps used in the manufacture of oncolytic vaccinia strains may result in viral preparations consisting primarily of the intracellular virus form of the virus. This implies that, without improvements in the manufacturing process, the advantages of EEV-enhancing mutations would only be experienced after initial infection of tumor cells and subsequent viral replication. Several strategies could be used to take advantage of this, such as initial direct injection of a primary tumor to allow subsequent spread to metastases or application of preinfected cells (e.g., tumor or immune cells) as a therapy.

The ability to improve spread within and between tumors and to enhance the delivery and movement of oncolytic viruses in immunized hosts represents a major step forward in the development of more effective oncolytic viruses.

Acknowledgments

References

1. Thorne SH, Hermiston T, Kirn D. Oncolytic virotherapy: approaches to tumor targeting and enhancing antitumor effects. Semin Oncol 2005;32: 537–48.
2. Parato KA, Senger D, Forsyth PA, Bell JC. Recent progress in the battle between oncolytic viruses and tumours. Nat Rev Cancer 2005;5:965–76.
3. Thorne SH, Hwang T-H, O'Gorman BE, et al. Rational strain selection and engineering creates a broad spectrum systemically effective oncolytic poxvirus JX-963. J Clin Invest 2007;117:3350–8.
4. Kim JH, Oh JY, Park BH, et al. Systemic armed oncolytic and immunologic therapy for cancer with JX-594, a targeted poxvirus expressing GM-CSF. Mol Ther 2006;14:361–70.
5. Buller RM, Palumbo GJ. Poxvirus pathogenesis. Microbiol Rev 1991;55:80–122.
6. Smith GL, Vanderplasschen A, Law M. The formation and function of extracellular enveloped vaccinia virus. J Gen Virol 2002;83:2615–31.
7. Smith GL, Symons JA, Khanna A, Vanderplasschen A, Alcami A. Vaccinia virus immune evasion. Immunol Rev 1997;159:137–54.
8. Ichihashi Y. Extracellular enveloped vaccinia virus escapes neutralization. Virology 1996;217:478–85.
9. Mathew EC, Sanderson CM, Hollinshead R, Smith GL. A mutational analysis of the vaccinia virus B5R protein. J Gen Virol 2001;82:1199–213.
10. McIntosh AA, Smith GL. Vaccinia virus glycoprotein A34R is required for infectivity of extracellular enveloped virus. J Virol 1996;70:272–81.
11. Parkinson JE, Sanderson CM, Smith GL. The vaccinia virus A38L gene product is a 33-kDa integral membrane glycoprotein. Virology 1995;214:177–88.
12. Law M, Hollinshead R, Smith GL. Antibody-sensitive and antibody-resistant cell-to-cell spread by vaccinia virus: role of the A33R protein in antibody-resistant spread. J Gen Virol 2002;83:209–22.
13. Carter GC, Rodger G, Murphy BJ, et al. Vaccinia virus cores are transported on microtubules. J Gen Virol 2003; 84:2443–58.
14. Blasco R, Sisler JR, Moss B. Dissociation of progeny vaccinia virus from the cell membrane is regulated by a viral envelope glycoprotein: effect of a point mutation in the lectin homology domain of the A34R gene. J Virol 1993;67:3319–25.
15. Thorne SH, Negrin RS, Contag CH. Synergistic antitumor effects of immune cell-viral biotherapy. Science 2006;311:1780–4.
16. Puhlmann M, Brown CK, Gnant M, et al. Vaccinia as a vector for tumor-directed gene therapy: biodistribution of a thymidine kinase-deleted mutant. Cancer Gene Ther 2000;7:66–73.
17. Yu YA, Shabahang S, Timiryasova TM, et al. Visualization of tumors and metastases in live animals with bacteria and vaccinia virus encoding light-emitting proteins. Nat Biotechnol 2004;22:313–20.
18. Bell E, Shamim M, Whitbeck JC, Sfyroera G, Lambris JD, Isaacs SN. Antibodies against the extracellular enveloped virus B5R protein are mainly responsible for the EEV neutralizing capacity of vaccinia immune globulin. Virology 2004;325:425–31.
19. Putz MM, Midgley CM, Law M, Smith GL. Quantification of antibody responses against multiple antigens of the two infectious forms of Vaccinia virus provides a benchmark for smallpox vaccination. Nat Med 2006;12: 1310–5.

AACR American Association for Cancer Research

Enhancing Poxvirus Oncolytic Effects through Increased Spread and Immune Evasion

David H. Kirn, Yaohe Wang, Wenchung Liang, et al.

Updated version	Access the most recent version of this article at: http://cancerres.aacrjournals.org/content/68/7/2071

Cited articles	This article cites 19 articles, 4 of which you can access for free at: http://cancerres.aacrjournals.org/content/68/7/2071.full#ref-list-1
Citing articles	This article has been cited by 9 HighWire-hosted articles. Access the articles at: http://cancerres.aacrjournals.org/content/68/7/2071.full#related-urls

E-mail alerts	Sign up to receive free email-alerts related to this article or journal.
Reprints and Subscriptions	To order reprints of this article or to subscribe to the journal, contact the AACR Publications Department at pubs@aacr.org.
Permissions	To request permission to re-use all or part of this article, use this link http://cancerres.aacrjournals.org/content/68/7/2071. Click on "Request Permissions" which will take you to the Copyright Clearance Center's (CCC) Rightslink site.